

A Model-based Reconstruction Technique for Parameter Mapping of Saturation Prepared Radially Acquired Data

Johannes Tran-Gia¹, Daniel Stäb¹, Dietbert Hahn¹, and Herbert Köstler¹
¹Institute of Radiology, University of Würzburg, Würzburg, Germany

Introduction

In MR parameter mapping, a suitable magnetization preparation is typically applied, followed by the acquisition of a certain number of images. In the presence of short relaxation times, sampling the signal evolution with multiple images is difficult or even impossible. The measurement has to be performed in a segmented fashion or with low spatial resolution. In this work we propose an iterative model-based image reconstruction algorithm in conjunction with radial data acquisition, capable of fully resolving an exponential signal evolution. Using an iterative fitting algorithm, one complete image is reconstructed for each single radial projection acquired after a saturation recovery (SR) magnetization preparation, thereby yielding the apparent relaxation parameters of the tissue.

Material and Methods

For every pixel, the signal $S(TI)$ after a SR magnetization preparation can be modeled by a mono-exponential function:

$$S(TI) = S_0 \cdot \left[1 - \exp\left(-\frac{TI}{T1_{eff}}\right) \right]$$

TI indicates the time after the saturation pulse, $T1_{eff}$ the apparent longitudinal relaxation time of the tissue in presence of RF excitation [1, 2, 3] and S_0 the steady state signal. Utilizing this model as prior knowledge allows characterizing $S(TI)$ by only the two parameters S_0 and $T1_{eff}$. By performing image acquisition with a radial trajectory, every acquired projection contains information about the image contrast. This information can be used in an iterative model-based image reconstruction to fully resolve the evolution of the signal with one image for each acquired radial projection, yielding S_0 and $T1_{eff}$ as results.

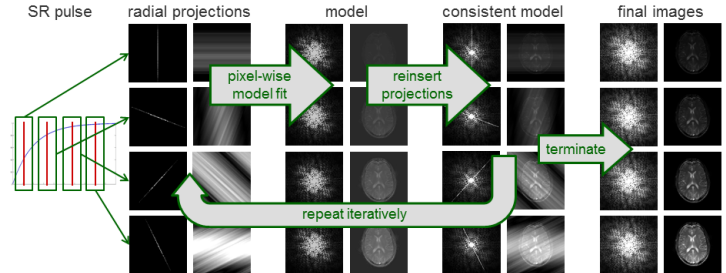


Fig. 1: Basic reconstruction scheme for 4 exemplary projections (red) acquired after an SR pulse (blue). Depicted are k-spaces (left) and image spaces (right) at different stages of the reconstruction process.

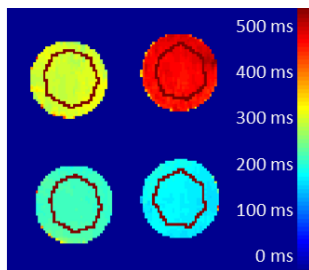


Fig. 2: Phantom measurements. $T1_{eff}$ map obtained using the proposed technique. The ROIs are indicated in dark red.

For image reconstruction, every single projection of the radially acquired k-space data was gridded onto the Cartesian grid using self-calibrating GROG [4] and Fourier transformed into image space. Subsequently, a least-squares fit was applied pixel by pixel, resulting in a set of parameters $S_0(x,y)$ and $T1_{eff}(x,y)$ for each pixel (x,y) , corresponding to model images for the contrast of each acquired projection. In order to ensure data consistency, each originally measured projection was substituted into the k-space of its model image. The consistent model images were then passed on to the following iteration (Fig. 1). The termination criterion was a minimum difference between model and consistent model.

Phantom and In-vivo experiments were carried out on a 3T whole-body scanner (Magnetom TRIO, Siemens AG Healthcare Sector, Erlangen, Germany) employing a 12 channel phased-array head coil for signal reception. The phantom experiments were performed on a phantom consisting of 4 compartments with different contrast agent (Gadovist, Bayer Schering Pharma, Berlin, Germany) concentrations using a Saturation Recovery FLASH sequence (FOV= 200 x 200 mm², TE = 3.15 ms, TR = 21.2 ms, flip angle 12°) with a Golden Ratio [5] radial k-space trajectory (1024 projections, 128 readout samples). 300 iterations of the proposed algorithm were utilized for image reconstruction and quantification of $T1_{eff}$. The resulting $T1_{eff}$ values were evaluated using a ROI analysis (Fig. 2). In order to assess the accuracy of the proposed algorithm, each of these vials was initially measured separately and reference values $T1_{ref}$ were determined.

position of compartment	$T1_{eff}$ (ms) reconstruction	$T1_{ref}$ (ms) reference
top right	448.8±8.3	456.3±4.2
top left	296.1±7.4	294.0±1.9
bottom left	223.0±3.6	218.5±1.7
bottom right	185.7±4.9	179.7±1.6

Table 2: Phantom measurements. $T1_{eff}$ values obtained using the proposed technique (center column) and by separate measurement of each vial (right column)

For the In-vivo measurements, a Saturation Recovery SSFP sequence (FOV = 260 x 260 mm², TE = 1.3 ms, TR = 10.4 ms, flip angle 50°, 512 projections, 128 readout samples) was utilized. For image reconstruction and estimation of the relaxation parameter $T1_{eff}$, 300 iterations of the proposed algorithm were executed.

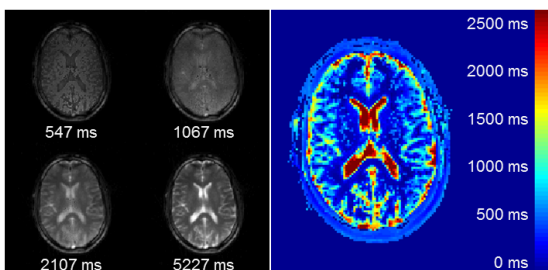


Fig. 3: In-vivo measurements. Reconstructed images for different contrasts TI (left) and $T1_{eff}$ map (right).

Results

Fig. 2 shows the $T1_{eff}$ map of the phantom, obtained using the proposed reconstruction algorithm as well as the ROIs used for the evaluation. The values of $T1_{eff}$ obtained in the ROIs (center column) and the values of the reference scans (right column) coincide within the measurement error (Table 1). Results of the in-vivo measurements are depicted in Fig. 3. Shown are exemplary images reconstructed from one single radial projection acquired at the times indicated after the SR magnetization preparation (left) as well as the corresponding $T1_{eff}$ map (right).

Discussion

The proposed model based algorithm allows quantifying relaxation parameters $T1_{eff}$ without the necessity of a compromise between temporal and spatial resolution. With one fully reconstructed image for every acquired radial projection, the method additionally provides an excellent temporal resolution of the signal recovery, which cannot be resolved using conventional reconstruction techniques such as inversion recovery snapshot FLASH [1]. The quality of the reconstructed images is comparable to a gridded mean image of all projections. However, an accurate model of the signal evolution is required in order to avoid systematic errors. The proposed technique is also suitable for mapping other parameters, like for example T2 decays.

References

- [1] Deichmann, J Magn Reson 96:608-612 (1992)
- [2] Scheffler, Magn Reson Med 49:781-783 (2003)
- [3] Schmitt, Magn Reson Med 51:661-667 (2004)
- [4] Seiberlich, Magn Reson Med 59:930-935 (2008)
- [5] Winkelmann, IEEE T Med Imaging 16:68-76 (2007)